A Metallurgical Characterization of HY-130 Steel Welds

Laser and electron beam welds in ¼ and ½ in. thick plate exhibit higher weld metal hardness and less susceptibility to cold cracking than do shielded metal arc and gas metal arc welds

BY J. STOOP AND E. A. METZBOWER

ABSTRACT. HY-130 steel weldments of 6.35 and 12.7 mm (¼ and ½ in.) thickness were fabricated by shielded metal arc (SMA), gas metal arc (GMA), electron beam (EB), and laser beam (LB) processes. Hardness explorations and metallographic examinations were made of the weld metal and heat-affected zone (HAZ) of the weldments. EB and LB weldments showed perceptibly higher weld metal hardnesses and steeper hardness gradients in the HAZ than corresponding SMA and GMA weldments.

SMA and GMA welds consisted of a large percentage of acicular ferrite with smaller amounts of bainite and martensite; EB and LB welds comprised mostly martensite and a small percentage of bainite.

As indicated by dynamic tear (DT) tests run at room temperature, the weld joint specimens exhibited mostly plane stress (slant) fracture. LB specimens disclosed a fracture toughness not only higher than that of the other weld joints but also comparable to the fracture toughness of the base metal.

Metallurgical conditions and variables that promote susceptibility to cold cracking were found to be more prevalent in SMA and GMA weldments than in EB and LB weldments. Inspection of the DT fractures disclosed a small to moderate amount of porosity in SMA and GMA weldments, the presence of cold shuts (incomplete fusion) in EB weldments, and some evidence on a minor scale of cold shuts and hydrogen embrittlement in the LB weldments.

Introduction

Quenched and tempered wrought HY-130 steel is a weldable high-strength material of exceptionally good resistance to fracture. In the welded condition, the steel can be made to equal or exceed the high yield strength and ultimate tensile strength it is capable of acquiring as a wrought or base metal. However, when welded by most fusion welding processes, the steel has a coarse, unworked, and partially refined structure. It, therefore, may not achieve fracture resistance and ductility properties equivalent to those of the base metal. Moreover, in the welded state, the steel may be especially susceptible to cold cracking in the weld metal and heat affected zone (HAZ).

Due to differences in basic welding techniques, variances in tensile properties, fracture resistance, and in hardness, as well as cold cracking susceptibility, may result from different welding methods such as the shielded metal arc (SMA), the gas metal arc (GMA), the electron beam (EB), and the laser beam (LB) processes. A better understanding of the metallurgical factors influencing these parameters in HY-130 weldments may contribute significantly to achieving fracture-safe structures with optimum mechanical properties and low susceptibility to cold cracking.

Essentially, the objective of this investigation was to explore and assess the mechanical properties and microstructural characteristics of HY-130 weldments fabricated by these fusion welding processes.

Paper presented at the AWS 59th Annual Meeting held in New Orleans, Louisiana, during April 3-7, 1978.

J. STOOP and E. A. METZBOWER are with the Material Science and Technology Division, Naval Research Laboratory, Washington, D. C.

Procedure

HY-130 weldments of 6.35 and 12.7 mm (¼ and ½ in.) thicknesses were fabricated by the SMA, GMA, EB, and LB processes. The weldments were examined for defects by radiographic inspection. Base and weld metal compositions are presented in Table 1; welding details are given in Tables 2 and 3.

Transverse cross sections were cut from the weldments for microhardness testing and metallographic examination. Cross sectional views of the weldments of 12.7 mm (½ in.) thickness are shown in Fig. 1. The weld configurations of the 6.35 mm (¼ in.) weldments were found to be similar to those shown in Fig. 1.

Hardness measurements were made in the mid-thickness region of the cross sections prepared for microexamination; a diamond pyramid indenter under a 300-gram load was used The measurements were begun at the center of the weld and extended across the weld and HAZ into the unaffected base metal. The Vickers hardnesses obtained were converted to the Rockwell C scale.

Transverse weld tension specimens were machined from the weldments for testing at room temperature. Base metal specimens of the same configuration also were prepared. This was done so that a basis for comparison could be made with the weld joint specimens. The base metal and weld joint specimens were machined with the longitudinal axes of the specimens aligned normal to the principal rolling direction of the plate.

Table 1—Base and Weld Metal Compositions of HY-130 Steel, WT-%

Sample thickness (mm)	C	S	P	Mn	Ni	Cr	Mo	Si	V	Cu	Ti	Al
Base metal (6.35)	0.11	0.005	0.005	0.80	4.70	0.60	0.54	0.21	0.07	0.06	0.004	0.05
Base metal (12.7)	0.085	0.007	0.006	0.74	4.70	0.52	0.54	0.22	0.07	0.19	0.003	0.05
SMA weld (6.35)	0.073	0.006	–	1.02	4.30	0.62	0.66	0.27	0.03	0.04	0.02	0.02
SMA weld (12.7)	0.064	0.008	0.009	1.05	4.00	0.60	0.95	0.29	0.02	0.06	0.02	0.02
GMA weld (6.35)	0.11	0.006	0.007	1.30	3.60	0.72	0.84	0.33	0.03	0.06	0.01	0.02
GMA weld (12.7)	0.10	0.006	0.007	1.42	3.15	0.74	0.81	0.35	0.02	0.08	0.02	0.02
EB weld (6.35)	0.11	–	–	0.85	4.80	0.62	0.59	0.26	0.07	0.08	0.004	0.03
EB weld (12.7)	0.079	–	–	0.70	4.75	0.55	0.52	0.24	0.07	0.18	0.005	0.05
LB weld (6.35)	0.115	–	–	1.00	5.00	0.47	0.56	0.26	0.08	–	–	0.02
LB weld (12.7)	0.076	–	–	0.96	5.00	0.45	0.54	0.25	0.08	–	–	0.03

Table 2—Welding Conditions for 6.35 mm Thick SMA, GMA, EB, and LB Weldments of HY-130 Steel

Parameter	SMA	GMA	EB	LB
Joint	60 deg V groove, 3.2 mm gap	60 deg V groove, 3.2 mm gap	Square butt	Square butt
Position	Flat	Flat	Flat	Flat
Filler metal	E14018, 4.0 mm diam electrode	140 S, 1.6 mm diam wire electrode	–	–
Amperage, A	125 DCRP	300 DCRP	0.184	–
Voltage, V	25-30	22.5-24.0	40,000	–
Power, kW	–	–	–	8-12
Passes	3	3	1	1
Travel speed, mm/s	3.7-4.2	8.9-9.7	29.8	23-25
Filler metal feed, mm/s	–	89	–	–
Environment	Gas + flux covering	Argon + 2% O_2 18.91/s	High vacuum	He
Preheat temperature, °C	≈ 120	≈ 120	–	–
Iterpass temperature, °C	95-150	95-150	–	–
Heat input, kJ/mm	0.81-0.93	0.77	0.25	0.34-0.47

Table 3—Welding Conditions for 12.7 mm Thick SMA, GMA, EB, and LB Weldments of HY-130 Steel

Parameter	SMA	GMA	EB	LB
Joint	60 deg V groove, 3.2 mm gap	60 deg V groove, 3.2 mm gap	Square butt	Square butt
Position	Flat	Flat	Flat	Flat
Filler Metal	E14018, 4.0 mm diam. electrode	140 S, 1.6 mm diam. wire electrode	None	None
Amperage, A	125 DCRP	300 DCRP	0.20–0.24	–
Voltage, V	25–30	23.5–24.5	40,000	–
Power, kW	–	–	–	10–11
Passes	7	5	1	1
Travel speed, mm/s	3.0	5.9–6.4	21.2	12.7–16.9
Filler metal feed, mm/s	–	89	–	–
Environment	Gas + flux covering	Argon + 2%O_2 18.91/s	High vacuum	He, argon
Preheat temperature, °C	≈ 120	≈ 120	None	None
Interpass temperature, °C	95-150	95-150	None	None
Heat input, kJ/mm	1.10–1.18	1.14–1.18	0.38–0.51	0.65–0.79

Dynamic tear (DT) base metal and weld joint specimens, both with the same configuration, were prepared for impact testing at room temperature in a double pendulum machine of 2712 N • m (2000 ft-lb) capacity. The DT weld joint specimens consisted of transverse cross sections from the different weldments. These were notched through the thickness along the centerline of the weld.

To avoid the possibility of buckling,

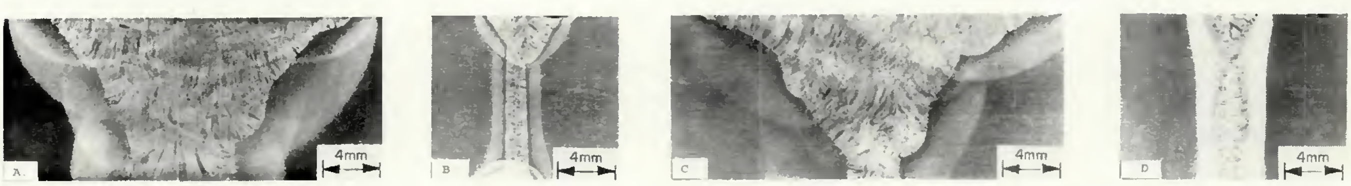

Fig. 1—Cross-sectional views of 12.7 mm thick HY-130 weldments etched in 10% ammonium persulphate: A—SMA weld; B—EB weld; C—GMA weld; D—LB weld

the specimens of 6.35 mm (¼ in.) thickness were laminated for testing in the two ply configuration. The DT weld joint and base metal specimens were machined with the notch aligned parallel (WR) to the principal rolling direction of the plates. Fractured DT specimens were subsequently replicated for transmission electron microscope (TEM) studies.

Results

Hardness and Microstructure

Hardness traverses which were made in the mid-thickness regions of the 6.35 and 12.7 mm thick weldments are plotted in Figs. 2 and 3, respectively. The traverses demonstrate hardness variations and gradients in the weld and heat-affected zones. Weld metal hardnesses are shown to be at a perceptibly higher level for the EB and LB welds than for the SMA and GMA welds. The gradients in the HAZ of the SMA and GMA weld joints are moderately steep and in most instances show

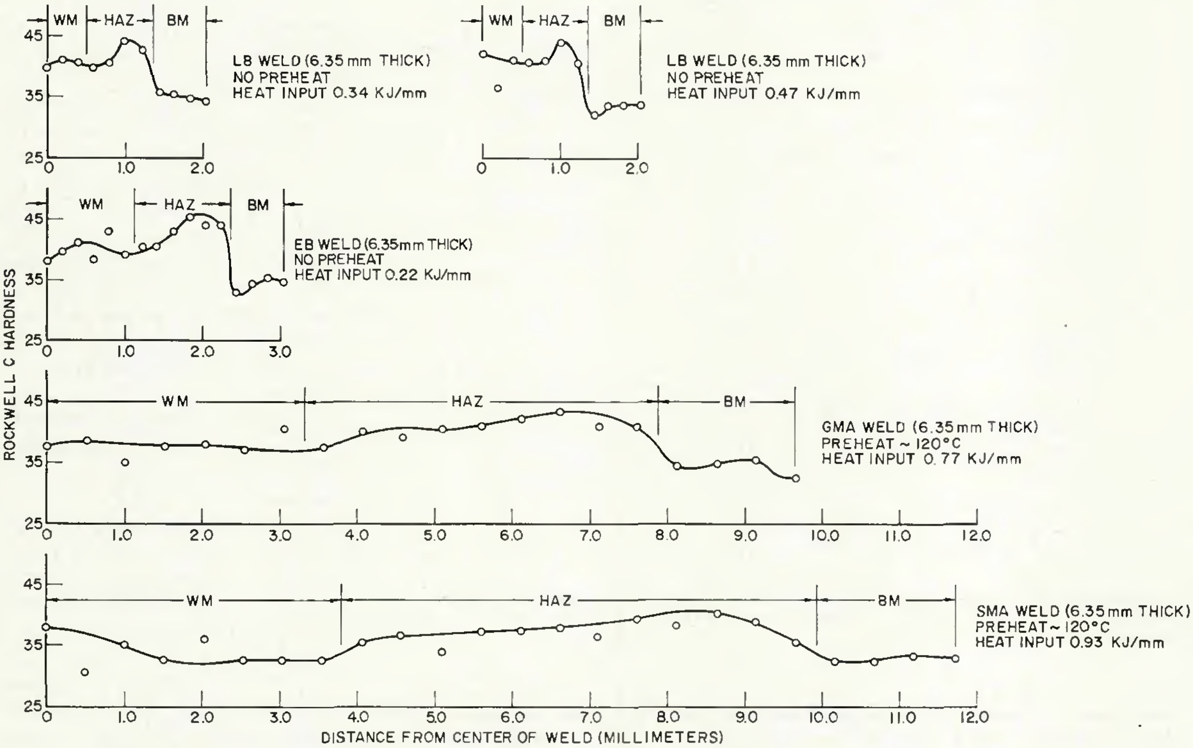

Fig. 2—Hardness traverses of 6.35 mm thick HY-130 SMA, GMA, EB, and LB weldments

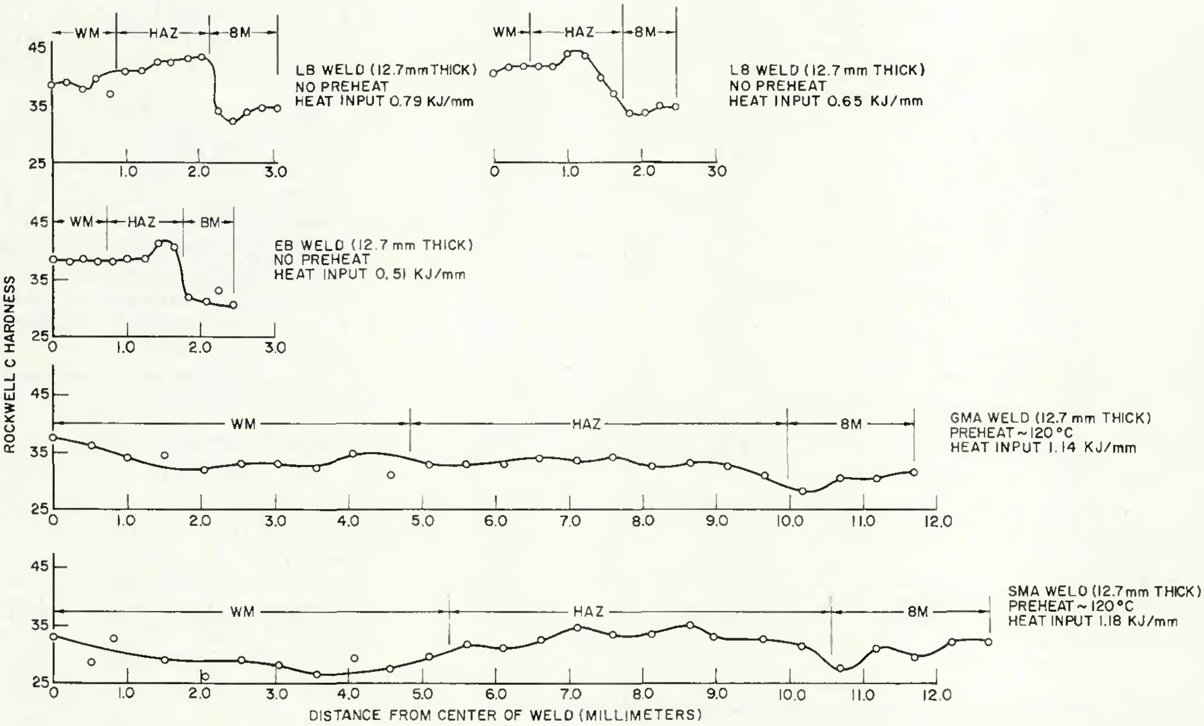

Fig. 3—Hardness traverses of 12.7 mm thick HY-130 SMA, GMA, EB, and LB weldments

Table 4—Microstructrues, Hardnesses, and Grain Sizes of 6.35 mm Thick Weldments

Weldment	Microstructure	Hardness, Rc	Grain size	Location
		Weld Metal		
SMA	Acicular ferrite + martensite	38.0	Largely very coarse	Center of weld
GMA	Acicular ferrite, martensite + bainite	37.5	Largely very coarse	Center of weld
EB	Martensite + some bainite	43.0	Medium-fine	0.8 mm from center of weld
LB	Martensite + some bainite	42.0	Largely fine	Center of weld
		Heat Affected Zone[a]		
SMA	Bainite	36.5	Coarse	1.0
SMA	Autotempered martensite + some ferrite	40.5	Fine	5.1
GMA	Bainite + some acicular ferrite	37.5	Coarse	0.5
GMA	Autotempered martensite + some ferrite	43.5	Fine	3.5
EB	Martensite + some bainite	40.5	Medium	0.2
EB	Martensite + some ferrite	45.5	Fine	0.8
LB	Martensite + some bainite	40.5	Medium	0.2
LB	Martensite + some ferrite	44.0	Fine	0.6

[a]Two areas of each weldment were examined: (1) the coarse grain region adjacent to the fusion boundary and (2) the fine grain region showing the highest hardness of the HAZ.

Table 5—Microstructures, Hardnesses, and Grain Sizes of 12.7 mm Thick Weldments

Weldment	Microstructure	Hardness, Rc	Grain size	Distance from center of weld, mm
		Weld Metal		
SMA	Acicular ferrite	26.0	Largely very coarse	2.0
GMA	Acicular ferrite	33.0	Largely very coarse	2.5
EB	Martensite + bainite	37.5	Medium-fine	0.4
LB	Martensite + bainite	38.5	Medium-fine	0.0
		Heat-affected zone[a]		
SMA	Bainite	31.5	Coarse	0.5
SMA	Autotempered martensite + ferrite	35.0	Fine	3.5
GMA	Bainite	33.0	Coarse	0.5
GMA	Autotempered Martensite + ferrite	34.0	Fine	3.0
EB	Martensite + some bainite	38.0	Medium	0.2
EB	Martensite + some ferrite	41.0	Fine	0.8
LB	Martensite + some bainite	41.0	Medium	0.4
LB	Martensite + some ferrite	43.5	Fine	1.2

[a]Two areas of each weldment were examined: (1) the coarse grain region adjacent to the fusion boundary and (2) the fine grain region showing the highest hardness of the HAZ.

a gradual decline in hardness from high hardness levels. The EB and LB weldments of 6.35 and 12.7 mm thickness, however, revealed noticeably steeper hardness gradients than the SMA and GMA weldments.

In the HAZ of both the 6.35 and 12.7 mm thick weldments, two regions were considered of significance from the standpoint of microstructure, hardness, and grain size:

1. The structure adjacent to the fusion boundary.
2. The fine-grain structure of highest hardness located most often beyond the midpoint of the HAZ.

The microstructural data of the weld metal and the aforementioned regions of the HAZ in the 6.35 and 12.7 mm thick weldments are compiled in Tables 4 and 5, respectively. Grain sizes in Tables 4 and 5 are expressed in relative terms such as fine, medium and coarse. Similarities in microstructure were found to exist between the SMA and GMA weldments of each thickness as well as between corresponding EB and LB weldments.

A series of microstructures illustrative of those from the various welding processes (SMA, GMA, EB, and LB) and the different positions in the weldments (weld metal, coarse grain region adjacent to the fusion zone and the fine grain region showing the highest hardness in the HAZ) are shown in Figs. 4-9.

The SMA welds were comparable to the GMA welds, and the EB welds to the LB welds. Nonetheless, some notable differences in microstructure were observed between similar welds. The EB welds of 6.35 mm thickness, for example, revealed a coarser solidification structure than the LB welds of the same thickness, as depicted in Figs. 10 and 11.

No significant differences in solidification structure were detected between the EB and LB welds of 12.7 mm thickness. The latter structures were comparable to the EB structures of the 6.35 mm thick weldments. At the weld metal-HAZ interface of the EB and LB weld joints, relatively fine microstructures were observed compared to the coarse weld metal-HAZ interface structure for the SMA weldment.

Tensile Properties

The tensile data of the base metal and transverse weld tension specimens of the 6.35 and 12.7 mm thick weldments are presented in Tables 6 and 7. The SMA weld joint specimens were the only ones which fractured in the weld metal. This was due to the lower tensile strength of the SMA weld compared with the tensile strength of the adjacent base metal. The specimens obtained from the 6.35 mm thick

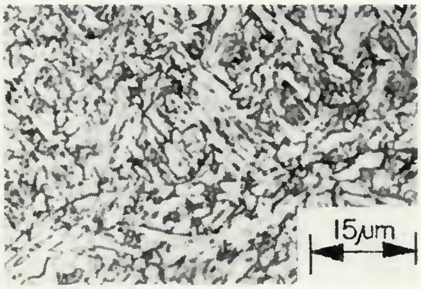

Fig. 4—Acicular ferrite in weld metal of 12.7 mm thick GMA weldment. Hardness—33.0 Rc. Etched in 1% nital

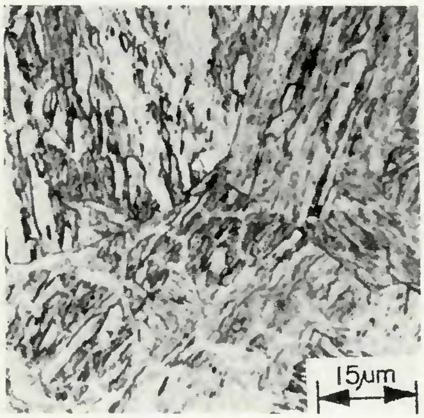

Fig. 5—Martensite and bainite in weld metal of 12.7 mm thick HY-130 LB weldment. Hardness—38.5 Rc. Etched in 1% nital

weldments in most instances revealed strength levels substantially higher than those of the 12.7 mm thick weldments. This was largely attributable to the higher hardenability of the 6.35 mm plates.

The SMA and GMA welds showed the lowest and highest values of yield strength, respectively, in both the 6.35 and 12.7 mm thicknesses. The yield strength ranges for these thicknesses were 799.1 to 1017.0 MPa (115.9 to 147.5 ksi) and 811.5 to 916.3 MPa (117.7 to 132.9 ksi). Although the EB and LB welds of 6.35 mm thickness revealed comparable yield strengths, the EB welds of 12.7 mm thickness disclosed a yield strength appreciably higher than that of the LB welds.

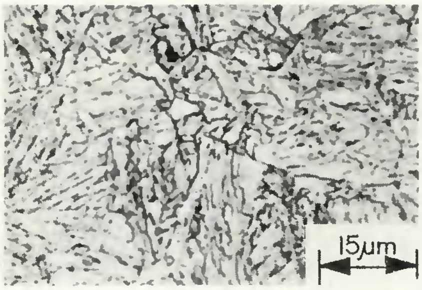

Fig. 6—Bainite in coarse grain region of HAZ adjacent to fusion boundary in 12.7 mm thick HY-130 GMA weldment. Hardness—33.0 Rc. Etched in 1% nital

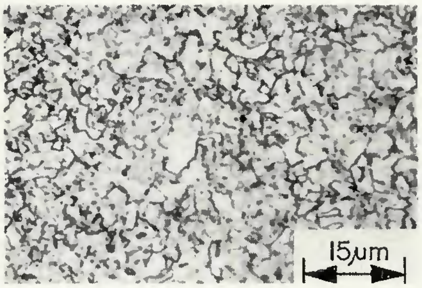

Fig. 7—Autotempered martensite and ferrite in fine grain region of HAZ in 12.7 mm thick HY-130 GMA weldment. Hardness—34.0 Rc. Etched in 1% nital

The 6.35 and 12.7 mm thick base metal plates differed significantly in their elongation and reduction of area. The especially high reduction of area for the 12.7 mm thick plates showed that considerable necking had taken place. The correspondingly high elongation measured for the material was not uniform and evidently was to a large degree attributable to the marked necking. Weld defects, particularly those related to porosity, contributed to low values of elongation and reduction of area in the SMA welds. This was especially evident in the 6.35 mm thick welds.

Fracture Resistance Properties

Fracture energy data for the 6.35 and 12.7 mm thick DT specimens are compiled in Tables 8 and 9. Presented

Fig. 8—Martensite and some bainite in medium grain region of HAZ adjacent to fusion boundary in 12.7 mm thick HY-130 LB weldment. Hardness—41.0 Rc. Etched in 1% nital

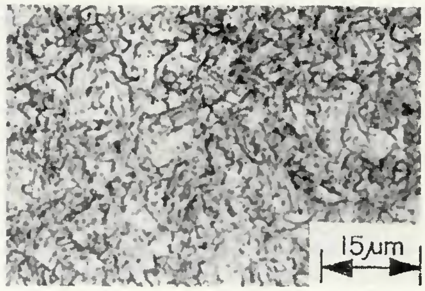

Fig. 9—Martensite and some ferrite in fine grain region of HAZ in 12.7 mm thick HY-130 LB weldment. Hardness—43.5 Rc. Etched in 1% nital

in the tables are DT energy, R_p, and average hardness values for the base metal and weld joint specimens. The R_p parameter provides an intrinsic and qualitative measure of the fracture toughness of the materials. The parameter was obtained from the empirical equation $E = R_p\ (\Delta a)^2 B^{1/2}$, where E is the fracture energy, Δa the fracture length, and B the thickness of the specimen (1). The R_p values in Tables 8 and 9, therefore, reveal in terms of a common denominator the variations in fracture resistance not only between the weld joint and base metal fracture of each thickness but also the markedly wide variations in fracture

Fig. 10—Solidification structure of weld metal at mid-thickness of 6.35 mm thick HY-130 EB weldment. Etched in 0.5% ammonium persulfate

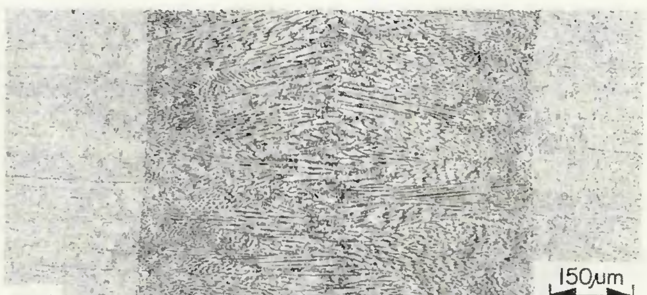

Fig. 11—Solidification structure of weld metal at mid-thickness of 6.35 mm thick LB weldment. Etched in 0.5% ammonium persulphate

Table 6—Average Tensile Properties of 6.35 mm Thick Weldments

Specimens	Fracture location	0.2% YS MPa	0.2% YS ksi	UTS[a] MPa	UTS[a] ksi	Elongation, %	Reduction of area, %	Hardness, Rc
Base metal	—	971.5	140.9	1014.3	147.1	13.3	63.3	34.0
SMA weld joint	Weld metal	799.1	115.9	997.0	144.6	7.2	42.8	33.5
GMA weld joint	Base metal	017.0	147.5	1019.8	147.9	10.3	58.9	37.5
EB weld joint	Base metal	994.3	144.2	1019.0	147.8	13.0	60.2	39.0
LB weld joint	Base metal	962.0	139.5	1022.1	148.2	12.6	62.0	40.0

[a]YS—yield strength; UTS—ultimate tensile strength.

Table 7—Average Tensile Properties of 12.7 mm Thick HY-130 Weldments

Specimens	Fracture location	0.2% YS[a] MPa	0.2% YS[a] ksi	UTS[a] Mpa	UTS[a] ksi	Elongation, %	Reduction of area, %	Hardness, Rc
Base metal	—	919.8	133.4	959.1	139.1	20.5	72.7	32.0
SMA weld joint	Weld metal	811.5	117.7	943.9	136.9	13.1	52.6	29.0
GMA weld joint	Base metal	916.3	132.9	955.6	138.6	17.0	73.1	34.0
EB weld joint	Base metal	909.5	131.9	946.0	137.2	18.5	74.2	38.0
LB weld joint	Base metal	846.5	122.8	960.3	139.3	18.9	74.3	40.0

[a]YS—yield strength; UTS—ultimate tensile strength.

resistance between the 6.35 and 12.7 mm thicknesses.

Examination of the fractures of the DT specimens (including the base metal specimens) revealed a large measure of plane stress (slant) fracture with flat fracture in the pop-in region and the area near the terminus of the fracture. In many cases small amounts of flat fracture were found to occur in the region midway between the pop-in and the fracture terminus. Fracture modes, in all instances, including fractures in the flat pop-in region of the weld metal, were identified as those of microvoid coalescence. Microvoid coalescence among the different weld joints generally showed variations in dimple size as indicated below:

1. SMA and GMA joint fractures (both thicknesses): medium to fine dimples in pop-in region; medium to coarse dimples in weld metal at midthickness; medium to fine dimples in weld metal near surface.
2. EB and LB weld joint fractures (both thicknesses): medium to coarse

Table 8—Fracture Resistance Data of 6.35 mm Thick HY-130 Weldments[a]

Specimens	DT energy range ft-lb	DT energy range N • m	Avg. DT Energy ft-lb	Avg. DT Energy N • m	R_p ft-lb / in. 5/2	R_p MN • m / m 5/2	Avg. hardness, Rc Weld metal	Avg. hardness, Rc HAZ
Base metal	342.0-415.0	464.0-563.0	391.0	530.0	437.1	5.8	34	
SMA weld joint	293.0-358.0	397.0-485.0	334.0	453.0	373.4	4.9	33.5	37.5
GMA weld joint	264.0-305.0	358.0-414.0	285.0	386.0	319.0	4.2	37.5	40.5
EB weld joint	267.0-348.0	362.0-472.0	308.0	418.0	344.3	4.5	39.5	43.0
LB weld joint	351.0-447.0	476.0-606.0	382.0	518.0	427.1	5.6	40.0	41.5

[a]Specimens were tested in a two-ply configuration of 6.35 mm thick laminates.

Table 9—Fracture Resistance Data of 12.7 mm Thick HY-130 Weldments

Specimens	DT energy range ft-lb	DT energy range N • m	Avg. DT energy ft-lb	Avg. DT energy N • m	R_p ft-lb / in. 5/2	R_p MN • m / m 5/2	Avg. Hardness, Rc Weld Metal	Avg. Hardness, Rc HAZ
Base metal	759.0-881.0	1029.0-1194.5	804.0	1090.0	899.0	11.9	32	
SMA weld joint	475.0-560.0	644.0- 759.0	524.0	710.5	586.0	7.7	29.0	33.0
GMA weld joint	420.0-633.0	569.5- 899.0	515.0	698.0	576.0	7.6	34.0	33.0
EB weld joint	585.0-634.0	793.0- 859.5	610.0	827.0	682.0	9.0	38.0	39.5
LB weld joint	567.0-948.0	769.0-1285.0	760.0	1030.0	850.0	11.2	40.0	41.0

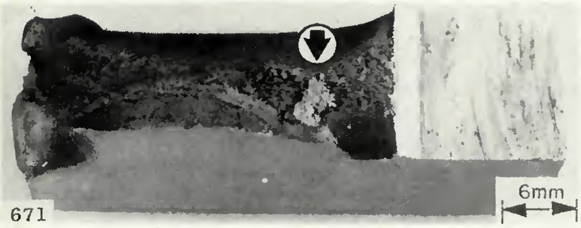

Fig. 12—Hydrogen flake in fracture surface of LB weld in 12.7 mm thick HY-130 DT specimen

Fig. 13 (right)—Enlarged view of flake (and surrounding area) in Fig. 12 showing: (left) highly fissured region below flake (center) and (right) pop-in region above flake

dimples in pop-in region; medium to fine dimples in weld metal at mid-thickness; mostly fine dimples in unaffected base metal.

Light fractographs revealed that the pop-in regions of the EB and LB weld joint fractures were similar in appearance to the pop-in regions of the base metal specimens. Evidence of gas pockets in the pop-in region of the EB weld was found. This type of porosity also was evident in the LB welds but to a more limited degree.

Of the 6.35 mm thick weld joints tested, the GMA and EB (preheated) specimens showed the lowest values of fracture resistance, as indicated in Table 8. The 6.35 mm thick SMA and GMA weld joints disclosed fractures of moderate porosity. The fractures had a somewhat sharp and irregular appearance. The low fracture resistance of the 6.35 mm thick GMA weld joints was believed attributable to porosity and the presence of a relatively high percentage of HAZ in the fracture. The unusually low fracture toughness found in the 6.35 mm thick EB specimens was due largely to the formation of cold shuts (incomplete fusion). These specimens, however, showed less evidence of porosity than the EB specimens of 12.7 mm thickness. The 6.35 mm thick LB weld joints revealed little porosity. Some evidence of incomplete fusion, however, was detected in one LB weld joint specimen.

Among the 12.7 mm thicknesses tested, the lowest values of fracture resistance were disclosed for the SMA and GMA weld joints—Table 9. Light to moderate porosity and a perceptible amount of flat fracture in the weld metal contributed in some measure to the low fracture toughness of these weld joints. The 12.7 mm thick EB weld joints showed evidence of more porosity and a greater degree of flat fracture than the corresponding LB weld joint specimens. Incomplete fusion also was found in the 12.7 mm thick EB weld joint specimens but to a more limited extent than in the EB specimens of 6.35 mm thickness.

The LB weld joints showed the highest average fracture resistance of the different weld joint specimens tested in both thicknesses. As shown in Tables 8 and 9, the fracture energies of the LB weld joints include values both higher and lower than average base metal values. In a comparable study, Breinan and Banas[2] found the fracture resistance of 6.40 mm thick HY-130 LB welds to be equivalent to or better than that of the base metal. They linked the high fracture toughness of the LB welds to a reduction of the inclusion content at the fusion zone.

A hydrogen flake was detected on the fracture surface of a dynamic-tear, 12.7 mm thick, LB weld joint specimen. The flake, shown in Figs. 12 and 13, was located in the weld metal between the pop-in region above it and a highly ruptured (porous) region below it. Transmission electron microscope (TEM) and scanning electron microscope (SEM) fractographs of the flake reveal evidence of intergranular fracture—Fig. 13. The fracture mode of the ruptured area below the flake is microvoid coalescence. The DT value (788 N • m) of the specimen was substantially below the average DT value (1030 N • m) for the 12.7 mm thick LB weld joint specimens.

Analysis of Results

The 6.35- and 12.7-mm base metal thicknesses revealed high yield strength: ultimate tensile strength (YS:UTS) ratios. However, since fracture took place in the base metal, no ultimate tensile strengths were obtained for the GMA, EB, and LB welds from the tests of the weld joint specimens.

It is not unusual to find marked variations in fracture resistance among different heats of wrought steel of the same chemical specifications. These variations can occur even though the materials are heat treated in the same way and notched similarly in regard to rolling direction.[3]

A wide divergence in fracture toughness is revealed between the 6.35 and 12.7 mm thick plates, as shown in Tables 8 and 9. The R_p parameter for the 12.7 mm thick base metal discloses an intrinsic fracture toughness one order of magnitude greater than that of the 6.35 mm thickness.

An interesting aspect of this disclosure is that the fracture toughnesses of the 12.7 mm thick weld joints differ from those of 6.35 mm thickness also by approximately one order of magnitude. It may be inferred from these R_p ratios that the quality of the weld joint from the standpoint of fracture resistance can be no better than that of the unaffected base metal. In most instances, the weld joint would not be expected to exceed the base metal in fracture resistance regardless of how low the fracture resistance of the plate might be.

The presence of high percentages of unaffected base metal in the fracture of the LB weld joints reasonably indicates that the greater share of the high fracture toughness of these weld joints was contributed by the unaffected base metal. This same trend in high fracture toughness should be manifested for the EB weld joints since these weldments also show fractures with high percentages of unaffected base metal. However, lower fracture toughnesses were obtained for the EB weld joints, particularly those of 6.35 mm thickness, due in large measure to the formation of cold shuts at the weld-HAZ interface. Such defects are difficult to detect by radiographic inspection.[4] The cold shuts represent, essentially, intrinsic cracks in the weld joints. With imposition of internal and external stresses; these cracks could very well propagate along the weld-HAZ interface. The cold shuts could also be sources of stress corrosion.[5]

Because of the small percentage of weld metal in the LB weld joint fractures, it is difficult to make a definite assessment of weld metal fracture toughness, but one can observe that the weld metal is at least comparable to the base metal in fracture toughness. Fractures of the LB weld joints correspond to upper shelf values on curves showing fracture energy and fracture mode transition temperatures. These upper shelf fractures portray the characteristic plane stress (slant fracture) configuration of ductile materials. If the LB weld metal does have greater fracture resistance than the base metal, it may be more effectively revealed by testing base metal and weld joint specimens over a range of temperatures (subzero to ambient temperatures). The fracture transition characteristics of the weld and base metals would be more selectively identified by such testing, especially at those temperatures where the metals are more conducive to plane strain (flat) fracture.

Potential sources of hydrogen that caused the flake found in the LB weld metal of the 12.7 mm thick dynamic tear specimen (Figs. 12 and 13) might be moisture adsorbed on the surface of the plates that were welded or possibly moisture contamination from the shielding gases. Hydrogen is believed to have been produced either by the dissociation of water vapor or more likely by the surface reaction of water vapor and metal (H_2O + $Fe \rightleftarrows FeO + 2H$). In this process liberated hydrogen was dissolved in the molten metal to form the flake which represents an area of high hydrogen concentration. The fissured region adjacent to the flake might be due to passage of water vapor, methane, or hydrogen sulphide through the melt. The gases could have been formed by reaction of excess hydrogen with oxygen, carbon, or sulphur in the metal.[6] Because of their insolubility in the melt, these gases could very likely have caused a severe bubbling or boiling action in the metal. That the fracture mode of this region was microvoid coalescence might indicate that there was little or no lattice absorption of hydrogen in the ruptured metal.

The metallurgical conditions and variables that promote susceptibility to cold cracking in the fabrication of HY-130 weldments are more prevalent in the multipass SMA and GMA weldments than in the single-pass EB and LB weldments. The SMA and GMA weldments are more likely to be subjected to a high degree of shrinkage distortion grain coarsening, and thermal cycling effects, which may create a wide coverage of residual stresses and sometimes high stress concentrations. When metal of limited ductility can no longer accommodate these stresses, the susceptibility to cold cracking may be very high. The EB and LB weldments will generally incur a minimum amount of distortion and shrinkage. The narrow weld and heat-affected zones of these weldments are of relatively high hardness and have grains that are medium to fine. Only a limited area for build-up of residual stresses is provided. Potential hydrogen absorptions may occur in all weldments and, with special emphasis on SMA weldments, can give rise to embrittlement and development of microcracks in weld metal and HAZ.

The hardness traverses for the SMA and GMA weld joints in Figs. 2 and 3 revealed no wide variations in hardness or steep hardness gradients.

In contrast, the EB and LB weld joints demonstrate high hardnesses and steep hardness gradients, which may indicate the presence of sizable stress concentrations. However, along with the high hardnesses in the latter weld joints, there is also a relatively fine grain size. The combination of high hardness and fine grain size constitutes what may be termed a beneficial synergistic effect, which imparts strength and toughness to the weld joints sufficient to withstand the build-up of high stresses. On the contrary, when high hardness is combined with a coarse grain size, then high stress concentrations can impose deleterious effects. Bernstein and Thompson[7] have shown that in low alloy steels resistance to hydrogen cracking is improved by a refined grain size and/or a tempered martensite structure.

Tempered bainite was revealed to be more susceptible to fracture than tempered martensite. Although tempering is not indicated in Tables 4 and 5, martensitic structures of the EB and LB weld joints were subjected to some degree of tempering at relatively low temperatures. This tempering action was due to heat developed in the welding operation.

In all weldment fabrications, regardless of the process used, susceptibility to cold cracking can be decreased substantially if the necessary precautions are taken in regard to the following items:

1. Cleanliness as related to grinding dust, flux entrapment, scale, oil, and grease.
2. Maintenance of proper preheating and interpass temperatures.
3. Effective moisture elimination from plates, covered electrodes, filler rod, and shielding gases.
4. Appropriate upkeep and utilization of welding equipment.

Summary of Results

1. Weldments of 6.35 mm (¼ in.) thickness were found to have somewhat higher hardness than weldments of 12.7 mm (½ in.) thickness because of the greater hardenability of the thinner plates. The EB and LB welds were perceptibly harder than the SMA and GMA welds. Average weld metal hardnesses of the SMA and GMA welds ranged from 29.0 to 37.5 Rc, and those of the EB and LB welds from 37.5 to 40.0 Rc. Hardness traverses across the heat-affected zones revealed noticeably steeper hardness gradients in the EB and LB weldments than in the SMA and GMA weldments.

2. The EB and LB welds showed relatively finer grain structures in the weld and HAZ than the SMA and GMA welds.

3. The microstructures of the SMA weldments were found to be similar to those of the GMA weldments. The EB and LB weldments were also similar in microstructure. The former microstructures consisted of a large percentage of acicular ferrite with somewhat smaller percentages of bainite and martensite, whereas the latter microstructures were composed mostly of martensite with smaller amounts of bainite.

4. Fracture of the SMA transverse weld tension specimens took place in the weld metal; the GMA, EB, and LB specimens fractured in the base metal. In both the 6.35 and 12.7 mm (¼ and ½ in.) thicknesses, the SMA welds showed the lowest yield strength values of 799.1 and 811.5 MPa (115.9 and 117.7 ksi). The GMA welds exhibited the highest yield strength values of 1017.0 and 916.3 MPa (147.5 and 132.9 ksi). The EB and LB yield strengths were at intermediate levels.

5. The DT fractures of the different weld joints, on the whole, revealed mostly plane stress (slant) fractures. However, SMA and GMA weld joints of 6.35 mm (¼ in.) thickness exhibited to a large degree fracture of somewhat sharp and irregular appearance.

6. The 6.35 and 12.7 mm (¼ and ½ in.) thick LB weld joint specimens showed the highest fracture toughness of all the weld joint specimens tested. As disclosed by examination of the fracture profiles of the specimens, the SMA and GMA fractures, in most instances, consisted predominantly of weld metal with a smaller percentage of HAZ. However, in the case of the EB and LB specimens, the fracture comprised largely unaffected base metal with smaller amounts of weld metal and HAZ. The high percentage of unaffected base metal in these fractures was a strong indication that the greater share of the EB and LB fracture toughnesses was attributable to this base metal component.

7. Metallurgical conditions and variables that promote susceptibility to cold cracking may be more prevalent in the SMA and GMA weldments than

in the EB and LB weldments. Some variables involved were hardness, stress, grain size, and microstructure. Deleterious effects of high hardness and steep hardness gradients in the EB and LB weldments may be offset by beneficial synergistic effects producing high hardness and a relatively fine grain size.

8. The SMA and GMA weldments showed no outright manifestations of hydrogen embrittlement but did reveal evidence of a relatively small to moderate amount of porosity. The most prominent defects observed in the EB weldments were cold shuts (incomplete fusion), whereas in the LB weldments there was evidence on a minor scale of incomplete fusion and hydrogen embrittlement.

Acknowledgments

The authors express their appreciation to Mr. D. A. Meyn for his assistance and guidance in strain gage instrumentation, and to Mr. E. R. Pierpoint for his fractographic work. We are especially grateful to the United Technologies Research Center for fabrication of the LB weldments.

References

1. Judy, Jr., R. W., and Griffis, C. A., "Fracture Extension Resistance of Aluminum Alloys in Thin Sections," NRL Report 7627, Oct. 12, 1973.

2. Breinan, E. M., and Banas, D. M., "Fusion Zone Purification During Welding with High Power CO_2 Lasers," United Aircraft Research Laboratories Report R111087-2, Apr. 1975.

3. Judy, Jr., R. W., and Goode, R. J., "Fracture Extension Resistance (R-Curve) Characteristics for Three High-Strength Steels," NRL Report 7361, Dec. 20, 1971, p. 5.

4. *Metals Handbook,* 8th ed., vol. 6, 1971, p. 539.

5. *Ibid.,* p. 288.

6. Linnert, G. E., ed., *Welding Metallurgy,* 3rd ed., 1967, vol. 2, p. 206, American Welding Society, Miami.

7. Bernstein, I. M., and Thompson, A. W., "Effect of Metallurgical Variables on Environmental Fracture of Steels," *International Metals Rev.,* 21, 278-279 (Dec. 1976).